Hardening behavior of an aluminum alloy in simple shear

F. Barlat[1,2], J.W. Yoon,[1,2]

Summary

Finite element (FE) simulations of the simple shear test were conducted for a 1050-O aluminum alloy sheet sample. The plastic anisotropy was accounted for using either a recently proposed anisotropic yield function combined with an isotropic strain hardening law or a crystal plasticity model. Experimental results conducted for this material sample in previous works were compared to the finite element predictions.

Introduction

In order to explore strain path changes that include forward and reverse loading (Bauschinger test) in thin sheet, simple shear was shown to be a versatile test[1]. In recent works, uniaxial tension and simple shear tests were conducted on a 1050-O aluminum alloy sheet sample[2, 3] in two specimen orientations, i.e., with shear at 45° and 90° from the rolling direction (RD). These tests showed that the hardening of the material was anisotropic, i.e., $d\sigma/d\varepsilon$ was orientation dependent, particularly after a strain path change. Even during monotonic loading, the strain hardening curves exhibited anisotropic behavior. It was shown that this behavior could be explained partially from crystallographic texture evolution, although the stress-strain curves predicted with crystal plasticity did not exhibit as much anisotropy as the experimental curves.

In this work, the influence of the boundary conditions on this anisotropic hardening behavior was investigated numerically for the 1050-O sheet sample. Finite element (FE) analyses were carried out using two different constitutive models, i.e., yield function with isotropic hardening and crystal plasticity. The predicted stress-strain curves were compared to experimental curves.

Material characterization and modeling

The crystallographic texture was characterized using orientation imaging microscopy (OIM). The resulting (111) pole figures (Fig. 1) indicated that the as-

[1] Materials Science Division, Alcoa Technical Center, 100 Technical Drive, Alcoa Center, PA 15069-0001, USA

[2] Center for Mechanical Technology and Automation, University of Aveiro, Aveiro 3810, Portugal

received materials exhibited a preponderant {100}<001> cube texture with different minor texture components.

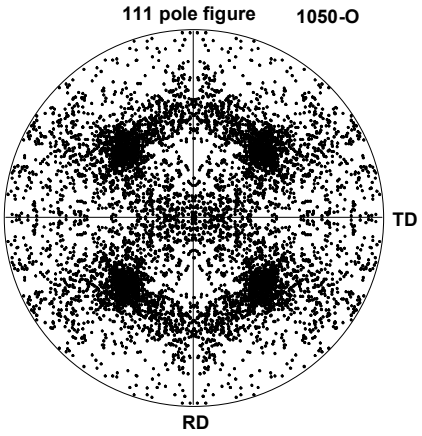

Fig. 1. (111) pole figure for 1050-O sheet sample

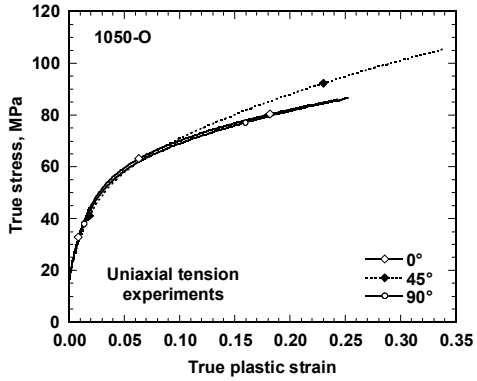

Fig. 2. Uniaxial stress-strain curves measured in different directions

In order to characterize the mechanical behavior, uniaxial tension tests in the rolling direction (RD), transverse direction (TD) and at 45° from the RD were conducted. Fig. 2 shows that the stress-strain curves measured in the RD and TD are identical. The flow curve measured at 45° from the RD is identical to that of the RD and TD curves up to a uniaxial strain of about 0.10. However, beyond this strain, the hardening rate ($d\sigma/d\varepsilon$ vs. ε) measured at 45° from the RD becomes higher than that of the RD and TD. Crystal plasticity calculations were able to reproduce this behavior semi-quantitatively. The stress-strain curve measured in the RD was approximated with the Swift law

$$\sigma = K\left(\varepsilon + \varepsilon_0\right)^n, \quad K = 132 \text{ MPa}, \ \varepsilon_0 = 0.0005 \text{ and } n = 0.285 \tag{1}$$

Tensile flow stresses and r values (width-to-thickness strain ratio) in the three orientations tested were used as input data to determine the coefficients of a recently developed yield function (Yld2004-18p). This yield function, which characterizes plastic anisotropy of aluminum alloy very well[4], is defined as

$$\begin{aligned}\phi = \phi(\boldsymbol{\Sigma}) = \phi\left(\tilde{\mathbf{S}}', \tilde{\mathbf{S}}''\right) = &\left|\tilde{S}_1' - \tilde{S}_1''\right|^a + \left|\tilde{S}_1' - \tilde{S}_2''\right|^a + \left|\tilde{S}_1' - \tilde{S}_3''\right|^a \\ + &\left|\tilde{S}_2' - \tilde{S}_1''\right|^a + \left|\tilde{S}_2' - \tilde{S}_2''\right|^a + \left|\tilde{S}_2' - \tilde{S}_3''\right|^a + \left|\tilde{S}_3' - \tilde{S}_1''\right|^a + \left|\tilde{S}_3' - \tilde{S}_2''\right|^a + \left|\tilde{S}_3' - \tilde{S}_3''\right|^a = 4\bar{\sigma}^a\end{aligned} \tag{2}$$

where $\bar{\sigma} = \mathrm{h}(\bar{\varepsilon})$ is a function of a measure of the accumulated plastic strain (hardening function). $\tilde{\mathbf{S}}'$ and $\tilde{\mathbf{S}}''$ represents the diagonal tensors associated with the principal values of two tensors $\tilde{\mathbf{s}}'$ and $\tilde{\mathbf{s}}''$, both defined as two linear transformations of the stress deviator **s**, i.e.,

$$\tilde{\mathbf{s}}' = \mathbf{C}'\mathbf{s} = \mathbf{C}'\mathbf{T}\boldsymbol{\sigma} = \mathbf{L}'\boldsymbol{\sigma}\,, \quad \tilde{\mathbf{s}}'' = \mathbf{C}''\mathbf{s} = \mathbf{C}''\mathbf{T}\boldsymbol{\sigma} = \mathbf{L}''\boldsymbol{\sigma} \tag{3}$$

$\mathbf{C}'$ and $\mathbf{C}''$ (or $\mathbf{L}'$ and $\mathbf{L}''$) contains eighteen constant anisotropy coefficients, which are consistent with the orthotropic material symmetry[4]. **T** transforms the stress tensor $\boldsymbol{\sigma}$ to its deviator **s**. In order to calculate the plastic strain increments, the associated flow rule is assumed.

Table 1

Mechanical anisotropy data 1050-O

$\sigma_0/\bar{\sigma}$	$\sigma_{45}/\bar{\sigma}$	$\sigma_{90}/\bar{\sigma}$	$\sigma_b/\bar{\sigma}$	r_0	r_{45}	r_{90}
1.000	1.000	1.000	0.999[3]	0.61	0.21	0.87

Table 2

Yld2004-18p coefficients for 1050-O (exponent a = 8)

c'_{12}	c'_{13}	c'_{21}	c'_{23}	c'_{31}	c'_{32}	c'_{44}	c'_{55}	c'_{66}
1.0943	1.2702	1.1276	0.79422	0.82939	7.7130	1.0048	1.2823	1.2823
c''_{12}	c''_{13}	c''_{21}	c''_{23}	c''_{31}	c''_{32}	c''_{44}	c''_{55}	c''_{66}
0.83005	0.85078	0.53708	0.75336	1.1192	1.0092	7.7176	1.0099	0.30279

The two linear transformations provide 18 coefficients that can be used to capture the material anisotropy. Based on crystal plasticity, Logan and Hosford[5] showed that in order to describe the behavior of BCC and FCC materials, the exponent *a* should be 6 and 8, respectively. In order to determine the coefficients for anisotropic materials, an error function was minimized using the steepest descent method. Details concerning the input data needed for the

[3] Computed from crystal plasticity

error function are given elsewhere[4]. The input data and resulting coefficients for the 1050-O sheet sample are given in Tables 1 and 2, respectively. As an application, the anisotropy of the 1050-O sheet sample is illustrated with the experimental and predicted variations of the normalized flow stress and r value as a function of the tensile direction (Fig. 3).

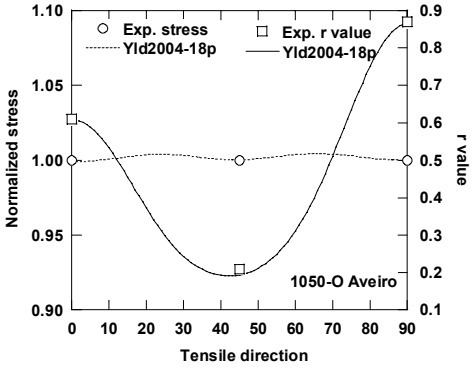

Fig. 3. Experimental and predicted anisotropy of the flow stress and r value

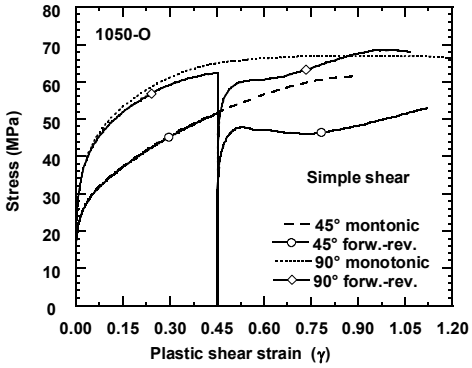

Fig. 4. Experimental monotonic and forward-reverse stress-strain curves in simple shear

Experimental and simulated simple shear tests

Simple shear tests were conducted for the 1050-O sheet sample in two specimen orientations[2, 3], i.e., with shear in the transverse direction (TD) or at 45° from the rolling direction (RD). The shear specimen size was 40 by 40 mm with a shear zone width of 8 mm and the thickness was 3 mm. More details concerning these tests were reported elsewhere[2, 3]. For monotonic loading, the experimental shear stress–shear strain curves along the two shear directions show that the material exhibits anisotropic strain hardening (Fig. 4). The strain hardening in the initial stage of plastic deformation is higher for simple shear in the TD but saturates prematurely compared to simple shear at 45° from the RD. For the forward-reverse test, the material yields prematurely upon reverse loading and, subsequently, exhibits a transient stage of lower hardening rate.

Finite element (FE) simulations were carried out using either the FE code MSC.MARC combined with the user constitutive material (HYPELA2) for Yld2004-18p described in the previous section, i.e., anisotropic yield function and isotropic hardening, or ABAQUS with UMAT for a rate-dependent crystal plasticity model [6]. The meshes, which were defined only for the shear

deformation zone of the specimens, contained four hundred elements for the simulations using the yield function and only one element for the simulations using crystal plasticity. As boundary conditions, one long side of the shear zone was assumed to be fixed while the other side was assumed to translate in a direction parallel to the fixed side.

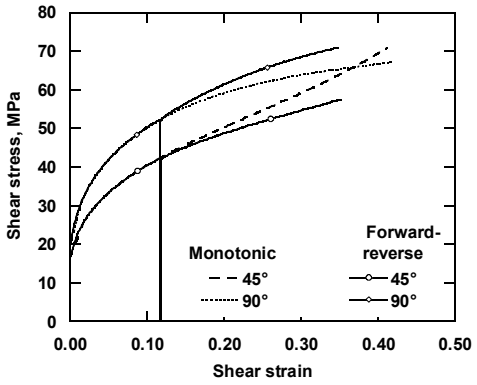

Fig. 5. Monotonic and forward-reverse stress-strain curves in simple shear predicted with yield function FE

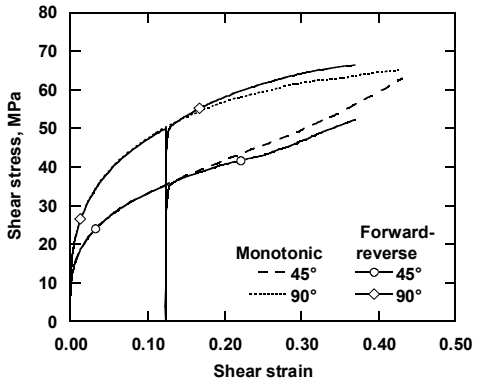

Fig. 6. Monotonic and forward-reverse stress-strain curves in simple shear predicted with crystal plasticity FE

The shear stress–shear strain curves along the two shear directions (at 45° from RD and in the TD), as predicted with Yld2004-18p (MSC.MARC) for the 1050-O sheet sample, are given in Fig. 5. For monotonic loading, although the material was assumed to exhibit isotropic hardening, the simulations were able to reproduce the anisotropic hardening observed experimentally during simple shear. For the forward-reverse sequences, the material yields when the reverse flow stress reaches the level of the monotonic curve. Beyond yield, the rate of strain hardening becomes different than that of the monotonic curve, i.e., larger for the 90° test and lower for the 45° test.

The simple shear stress-strain curves predicted with crystal plasticity (ABAQUS UMAT) for the 1050-O sheet sample are shown in Fig. 6. Qualitatively, the results are identical to those obtained with the yield function.

Discussion

Experimental and predicted shear flow curves exhibit clear differences in hardening behavior $d\sigma/d\varepsilon$ depending on the testing direction. In previous works

[2, 3], crystal plasticity simulations demonstrated that these differences could be explained, at least partially, by crystallographic texture evolution. Based on more realistic boundary conditions, the above FE analysis shows that, in spite of the isotropic hardening assumption, the stress-strain curves exhibit an apparent anisotropic strain hardening. One possible reason to explain this phenomenon is that a simple shear strain applied to an anisotropic material results not only in a shear stress but also in a normal stress in the direction orthogonal to shear. In the current calculations, it was found that the normal stresses for simple shear at 45° from the RD and in the TD are of opposite sign. This means that the combined loadings for the two test directions are different, i.e., the functioning points on the yield surfaces are different and lead to apparent anisotropic hardening.

For monotonic loading, the combination of the boundary condition effect, which produces an apparent anisotropic hardening, and texture evolution, which leads to a real anisotropic hardening effect, can fully explain the behavior of the 1050-O sheet sample deformed in simple shear. However, for forward-reverse loading sequences, the transient flow behavior cannot be explained in terms of crystal plasticity and boundary conditions only. Other features, such as dislocation structures, play an important role. Nevertheless, this analysis points out the need for a better method to characterize strain hardening in simple shear from the experimental data, in order to eliminate "apparent effects."

References

1 Rauch, E.F., Schmitt, J.-H., 1989. Dislocations substructures in mild steel deformed in simple shear. *Mater. Sci. Eng*. A113, 441-448.

2 Lopes, A.B., Barlat, F., Grácio, J.J., J. Ferreira Duarte, Rauch, E.F., 2003. Effect of texture and microstructure on strain hardening anisotropy for aluminum deformed in uniaxial tension and simple shear. *Int. J. Plasticity* 19, 1-22.

3 Barlat, F., Ferreira Duarte, J., Gracio, J.J., Lopes, A.B., Rauch, E.F., 2003. Plastic flow for non-monotonic loading conditions of an aluminum alloy sheet sample. *Int. J. Plasticity* 19, 1215-1244.

4 Barlat, F., Aretz, H., Yoon, J.W., Karabin, M.E., Brem, J.C., Dick, R.E., 2004. Linear transfomation-based anisotropic yield functions. Submitted for publication in *Int. J. Plasticity*.

5 Logan, R.W., Hosford, W.F., 1980. Upper-bound anisotropic yield locus calculations assuming pencil glide. *Int. J. Mech. Sci.* 22, 419–430.

6 Dao, M., Asaro, R.J., 1996. Localized deformation modes and non-Schmid effects in crystalline solids. Part I. Critical conditions of localization. *Mech. Mater.* 23, 71-102.